Theoretical Chemistry Accounts (2024) 143:36
https://doi.org/10.1007/s00214-024-03113-0

RESEARCH

First-principles calculations on the structures and electronic properties of the TMW_2O_n (TM = Mn–Ni, n = 1–6) clusters

Zhi Li[1] · Zi-hao Wu[1] · Zhen Zhao[2]

Received: 11 January 2024 / Accepted: 1 April 2024 / Published online: 12 April 2024

Abstract

Transition metals can enhance the electronic attributes of tungsten oxides. In this study, we focused on W_2O_n (n = 1–6) clusters as a representative examples of tungsten oxide clusters with varying oxygen concentrations. The structures and electronic properties of the $TMWO_n$ (TM = Mn–Ni) clusters have been calculated using first-principles. The ground-state $TMWO_n$ clusters share some structural similarities with the ground-state W_2O_n (n = 1–6) clusters. The W–O bonds of the $TMWO_2$ (TM = Fe–Ni) clusters are significantly distorted into a triangular structure. The $NiWO_n$ (n = 1–2) and $CoWO_n$ (n = 3–5) clusters display greater thermodynamic stability than other $TMWO_n$ clusters. Among the $TMWO_n$ clusters, the W_2O_4, W_2O_6, MnWO, $MnWO_3$, $MnWO_6$, FeWO, $FeWO_4$, $FeWO_6$, CoWO, $CoWO_6$, $NiWO_2$, $NiWO_5$ clusters are more kinetically stable. Furthermore, the amount of charge transfer between the TM atoms and W_2O_n clusters increases from 0.050 |e| to 1.066 |e| as the number of oxygen atoms increases. The 4*s* orbital electrons of the TM atoms for the $TMWO_n$ clusters are partially transferred to the neighboring O atoms.

Keywords Tungsten trioxide clusters · First-principles · Structures · Electronic properties

1 Introduction

Tungsten oxides (WO_3) are important materials with a variety of industrial applications, including electrochromic devices, chemical sensors, dye-sensitized solar cells, and catalysts etc. [1, 2]. Due to the similarity of the chemical bond formed on the WO_3 surface to a cluster-like bond, investigating WO_3 clusters can provide insight into the properties of bulk surfaces [3]. In fact, the WO_3 clusters have been observed experimentally on the surfaces of WO_3 films [4, 5]. Theoretical investigations on the WO_3 clusters have also been extensively conducted. For example, Li et al. [6] have investigated the ground-state structures of the $(WO_3)_n$ (n = 1–6) clusters using the B3LYP gradient-corrected exchange–correlation functional. Sai et al. [1] have investigated the ground-state structures of the $(WO_3)_n$ ($2 \le n \le 12$) clusters using first-principles. These studies have revealed that the WO_3 clusters exhibit unique electronic, magnetic, and chemical properties compared to bulk materials [7]. It is important to note that the WO_3 clusters contain both terminal and bridging O atoms, except for the smallest WO_3 molecule [3]. On the other hand, to highlight the influence of oxygen concentrations on the electronic properties of tungsten oxide clusters, some studies have been performed. Such as, Zhai et al. [8] have investigated the electronic structures and chemical bonding of WO_n and WO_n^- species (n = 3–5) using anion photoelectron spectroscopy (PES) and density functional theory (DFT) calculations. Huang et al. [9] have investigated the electronic structure and chemical bonding of the $W_3O_n^-$ and W_3O_n (n = 7–10) clusters. Zhai et al. [10] have investigated the electronic structures and chemical bonding of the $W_2O_n^-$ and W_2O_n (n = 1–6) using PES and DFT calculations. However, the larger band gap of the WO_3 clusters restricts their potential applications [10, 11]. To address this issue, various methods have been considered to reduce the energy gap, including transition metal doping [12]. For example, Zhao et al. [13] have investigated the structures, electronic and magnetic properties of the $TM@W_6O_{18}$ clusters using DFT. Hameed et al [14] have

✉ Zhi Li
lizhi81723700@163.com

[1] School of Materials and Metallurgy, University of Science and Technology Liaoning, PO Box 114051, Anshan, People's Republic of China

[2] School of Chemistry and Life Science, Anshan Normal University, PO Box 114007, Anshan, People's Republic of China

investigated the influence of the TM (TM = Fe–Zn) concentrations on the catalytic properties of WO_3 nanoparticles using ultraviolet laser irradiation. Mansouri et al. [15] have investigated the effect of TM substitution and vacancies the in WO_3 crystal using Ab Initio method. However, no reports on the electronic properties of the TM substituted small tungsten oxide clusters with different oxygen concentrations.

In this study, to highlight the influence of oxygen concentrations on the electronic properties of magnetic TM-substituted tungsten oxide clusters, the structures, electronic properties and dipole magnitudes of the $TMWO_n$ (TM = Mn–Ni, n = 1–6) clusters have been investigated using DFT.

2 Computational details

The ground-state structures of the W_2O_n (n = 1–6) clusters were obtained from Ref. [10]. Then a W atom of the W_2O_n clusters was substituted by a TM (TM = Mn–Ni) atom to construct the hypothetical $TMWO_n$ clusters. The geometry optimization and property calculations were executed using the DMol^3 software [16, 17]. The generalized gradient approximation (GGA) and Perdew-Burke-Ernzerhof (PBE) were adopted to consider exchange-correction interaction [1, 18]. The structures of the $TMWO_n$ clusters were optimized without any symmetry constraints [1, 7]. Spin unrestricted was chosen [1, 13, 19]. All electron relativistic calculations were adopted to account for electron–ion interactions, as W is a heavy element [1, 19]. Double numerical plus polarization (DNP) was considered for each atom [19]. Mülliken population analysis was performed to obtain the net charge of each atom [20]. Harmonic vibrational analysis of the frequencies of the $TMWO_n$ clusters was executed to ensure the presence of saddle points on the potential energy surfaces [1, 21, 22]. It has been confirmed that there are no imaginary frequencies of the $TMWO_n$ clusters. The convergence thresholds for self-consistent field calculations were set: 1×10^{-5} Hartree/Bohr for the energy gradient, 2×10^{-3} Hartree/Å for the maximum force and 5×10^{-3} Å for the atomic displacement, respectively. For total energy convergence, the threshold was set at 1×10^{-5} Hartree, and for charge density, it was set at 1×10^{-6} e/Å^3. The width of smearing was selected as 0.005 eV and the project out zero frequency modes option was selected.

The binding energies per atom of the W_2O_n (n = 1–6) and $TMWO_n$ (TM = Mn–Ni, n = 1–6) clusters were calculated to investigate their thermodynamic stability [13]

$$E_b = [2E(W) + nE(O) - E(W_2O_n)]/(2+n) \quad (1)$$

$$E_b = [E(TM) + E(W) + nE(O) - E(TMWO_n)]/(2+n) \quad (2)$$

where E(W), E(O) and E(TM) represent the atomic energies of single W, O and TM, respectively. $E(W_2O_n)$ and $E(TMWO_n)$ represent the total energies of W_2O_n and $TMWO_n$ clusters, respectively.

The temperature dependence of the free energy of the ground-state W_2O_n (n = 1–6) and $TMWO_n$ (TM = Mn–Ni, n = 1–6) clusters [23]

$$F(T) = E_{tot} + \frac{1}{2}\int F(\omega)h\omega d\omega + kT\int F(\omega)\ln\left[1-\exp\left(-\frac{h\omega}{kT}\right)\right]d\omega \quad (3)$$

where the second item is the zero point vibrational energy, k is Boltzmann constant, h is Planck constant and $F(\omega)$ is the phonon density of states. Due to the change of $P\Delta V$ is rather small under constant pressure, F is approximately equal to the Gibbs free energy G.

To ensure the accuracy of the selected PBE functional, the calculated bond length (1.757 Å) and the binding energy (1.082 eV) of WO_3 clusters were compared to the corresponding calculated values (1.752 Å and 1.10 eV) [7]. Similarity, the calculated bond length (1.619 Å) and binding energy (4.180 eV) of FeO molecules were compared to experimental results (1.62 Å and 4.17 eV) [24]. These comparisons demonstrate the suitability of the PBE functional for calculating $TMWO_n$ clusters.

3 Results and discussion

3.1 Structures

The binding energies per atom E_b have been used to determine the lowest-energy configurations of the $TMWO_n$ (TM = Mn–Ni, n = 1–6) clusters. Only the ground-state configurations of the calculated $TMWO_n$ (TM = Mn–Ni, n = 1–6) clusters have been shown in Fig. 1. It is worth noting that the lowest-energy structures of the $TMWO_n$ clusters are largely inherited from those of the W_2O_n (n = 1–6) clusters. However, the point groups of the $TMWO_n$ clusters exhibit a degeneracy, resulting in an asymmetric structure C_1. Compare these $TMWO_n$ clusters, it can be found that the sizes of TM atoms have less effect on the tungsten oxide structures [25]. For instance, in the case of the $TMWO_2$ (TM = Fe–Ni) clusters, the W–O bonds are significantly distorted into a triangular structure due to the influence of TM-*d* electrons, leading to the Jahn–Teller distortion [8, 21]. Zhao et al. [13] have also found that the structural distortions of the $Co@W_6O_{18}$ clusters using DFT.

3.2 Stabilities

The calculated binding energies per atom E_b of W_2O_n and $TMWO_n$ (TM = Mn–Ni, n = 1–6) clusters have been

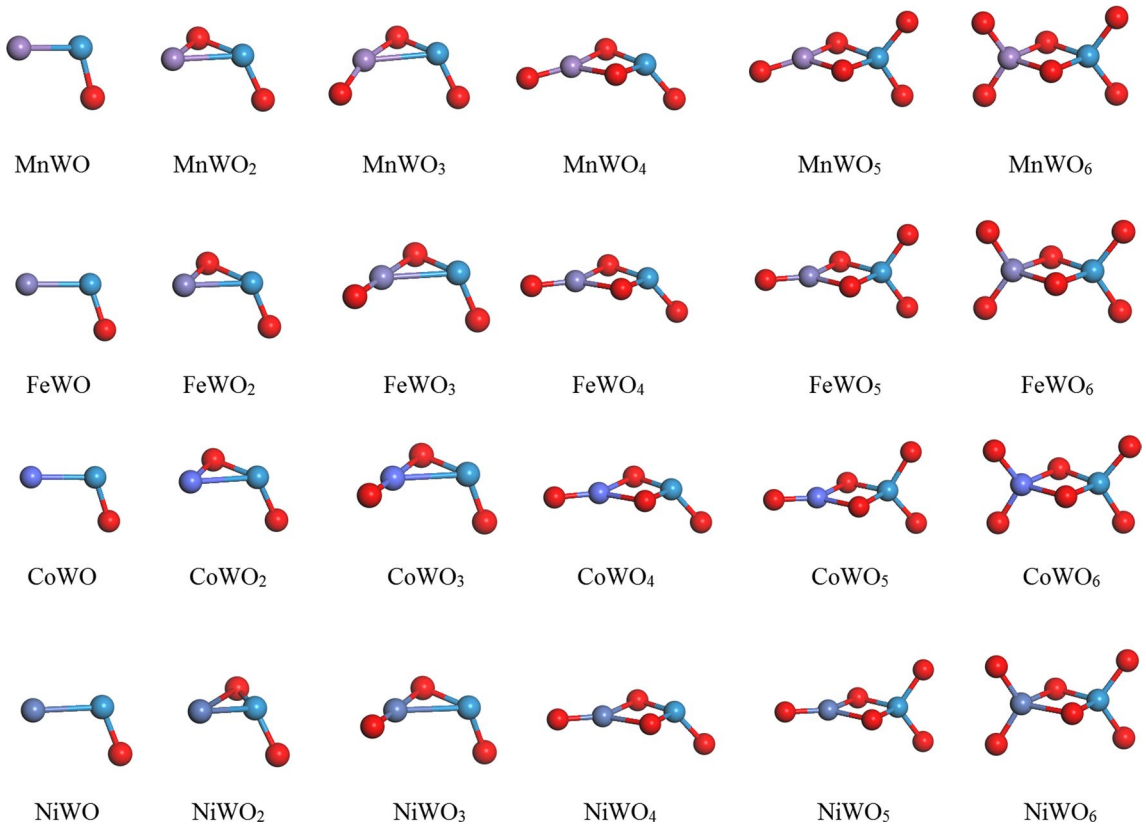

Fig. 1 Ground-state structures of the $TMWO_n$ (TM = Mn, Fe, Co and Ni, n = 1–6) clusters

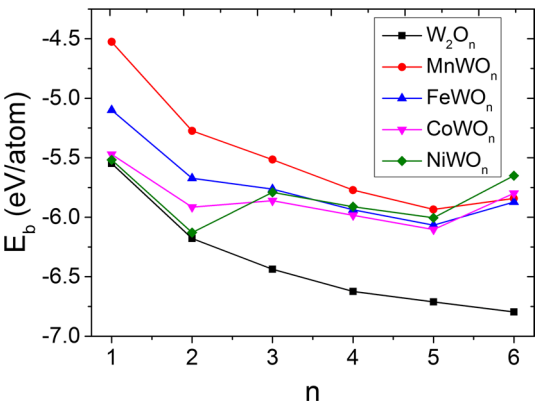

Fig. 2 Binding energies per atom of pristine W_2O_n and $TMWO_n$ (TM = Mn, Fe, Co and Ni, n = 1–6) clusters

exhibited in Fig. 2. The more the negative binding energies, the more the stability will be [26]. The binding energies per atom of the W_2O_n clusters decrease with the increase of O concentrates. Wang et al. [27] have revealed that more O atoms prefer to firm W atoms. When comparing the binding energy per atom of the W_2O_n clusters to the $TMW_{n-1}O_{3n}$ clusters, it is evident that the W_2O_n clusters have lower binding energies per atom. This indicates that the W_2O_n clusters are less thermodynamically stable. When comparing the different $TMWO_n$ clusters, it can be observed that the $NiWO_n$ (n = 1–2) clusters display greater thermodynamic stability than the other $TMWO_n$ (TM = Mn, Fe and Co, n = 1–2) clusters. This is likely due to the ability of these clusters to maximize the coordination number of the surface atom [28], as well as the strong binding of oxygen-2p electrons [8, 9]. Similarly, the $CoWO_n$ (n = 3–5) clusters exhibit more thermodynamic stability than the other $TMWO_n$ (TM = Mn, Fe and Ni, n = 3–5) clusters. On the other hand, the $FeWO_6$ clusters show more thermodynamic stability than the other $TMWO_6$ (TM = Mn, Co and Ni) clusters. This is mainly due to differences in the electron affinity of the TM atoms [29, 30].

The structure distortions should lead to the electron redistributions [31]. The calculated gaps between the highest molecular occupied orbital (HOMO) and the lowest molecular unoccupied orbital (LUMO) states of the W_2O_n and $TMWO_n$ (TM = Mn–Ni, n = 1–6) clusters have been plotted in Fig. 3. The calculated values of the HOMO–LUMO gaps are determined by the basis set [2], but it is still possible to investigate the relative electronic stability of the W_2O_n and $TMWO_n$ clusters. According to previous research, the

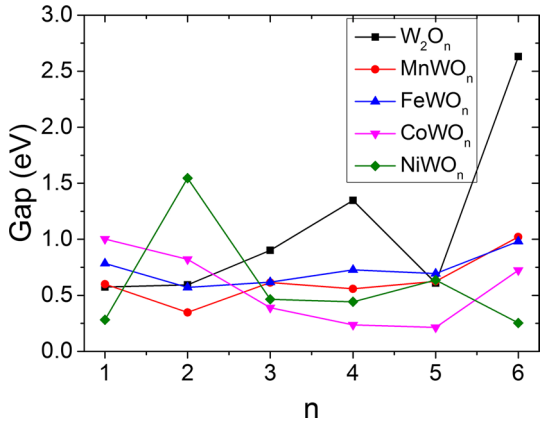

Fig. 3 HOMO–LUMO gaps of pristine W_2O_n and $TMWO_n$ (TM = Mn, Fe, Co and Ni, n = 1–6) clusters

clusters with larger HOMO–LUMO gaps tend to be more stable and chemically inert [13]. Among the clusters studied, the W_2O_4, W_2O_6, MnWO, $MnWO_3$, $MnWO_6$, FeWO, $FeWO_4$, $FeWO_6$, CoWO, $CoWO_6$, $NiWO_2$, $NiWO_5$ clusters display higher kinetic stability compared to their neighboring $TMWO_n$ clusters. On the other hand, the W_2O, W_2O_5, $MnWO_2$, $MnWO_4$, $FeWO_2$, $FeWO_5$, $CoWO_5$, NiWO, $NiWO_4$, $NiWO_6$ clusters exhibit higher kinetic activity. This can be attributed to the distortion of the HOMO mainly on the O sites and the LUMO mainly on the W atoms. These results are a result of the distortion of the atoms and charge redistribution near the atoms [18].

Clusters with both good structural and thermodynamic stability tend to be synthesized experimentally. The $NiWO_n$ (n = 1–2) and $CoWO_n$ (n = 3–5) clusters display greater thermodynamic stability than other $TMWO_n$ clusters. The MnWO, $MnWO_3$, $MnWO_6$, FeWO, $FeWO_4$, $FeWO_6$, CoWO, $CoWO_6$, $NiWO_2$, $NiWO_5$ clusters display higher kinetic stability compared to their neighboring $TMWO_n$ clusters. It indicates that the $NiWO_2$ and $CoWO_6$ clusters prefer to synthesize.

The HOMO and LUMO orbitals of the W_2O_n and $TMWO_n$ (TM = Mn–Ni, n = 1–6) clusters have been depicted in Figs. 4 and 5. In the HOMO states of the $TMWO_n$ clusters, there are more electrons surrounding the TM atoms, except for the NiWO, $FeWO_2$, $CoWO_2$ clusters. Similarly, in the LUMO states of the $TMW_{n-1}O_{3n}$ clusters, there are more electrons surrounding the TM atoms, except for the NiWO, $FeWO_2$, $CoWO_2$, $NiWO_2$, $CoWO_3$, $NiWO_3$, $MnWO_4$, $CoWO_4$ clusters [21, 32]. The HOMO and LUMO states of the $TMWO_n$ clusters, σ-type bonds and π-type bonds are coexist [32]. This can be attributed to the contributions of TM-*d* and O-*p* orbital electrons [1, 25, 33, 34].

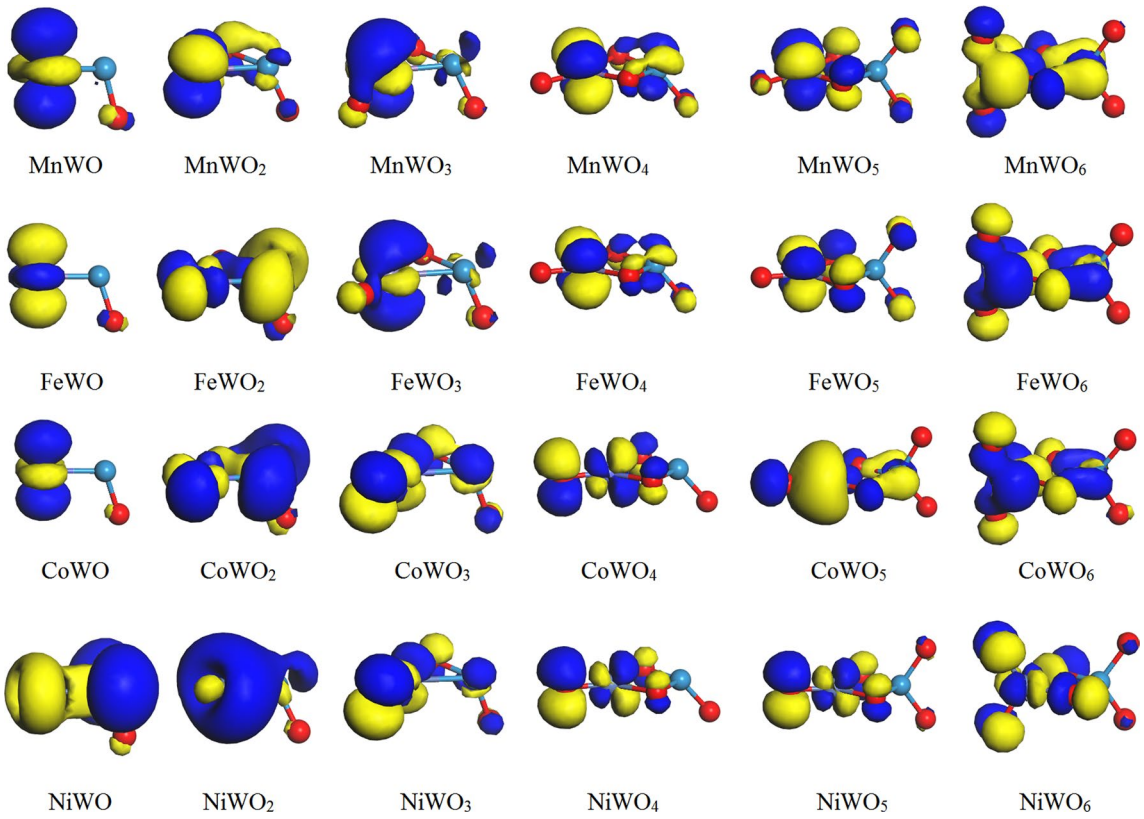

Fig. 4 HOMO orbitals of the $TMWO_n$ (TM = Mn, Fe, Co and Ni, n = 1–6) clusters

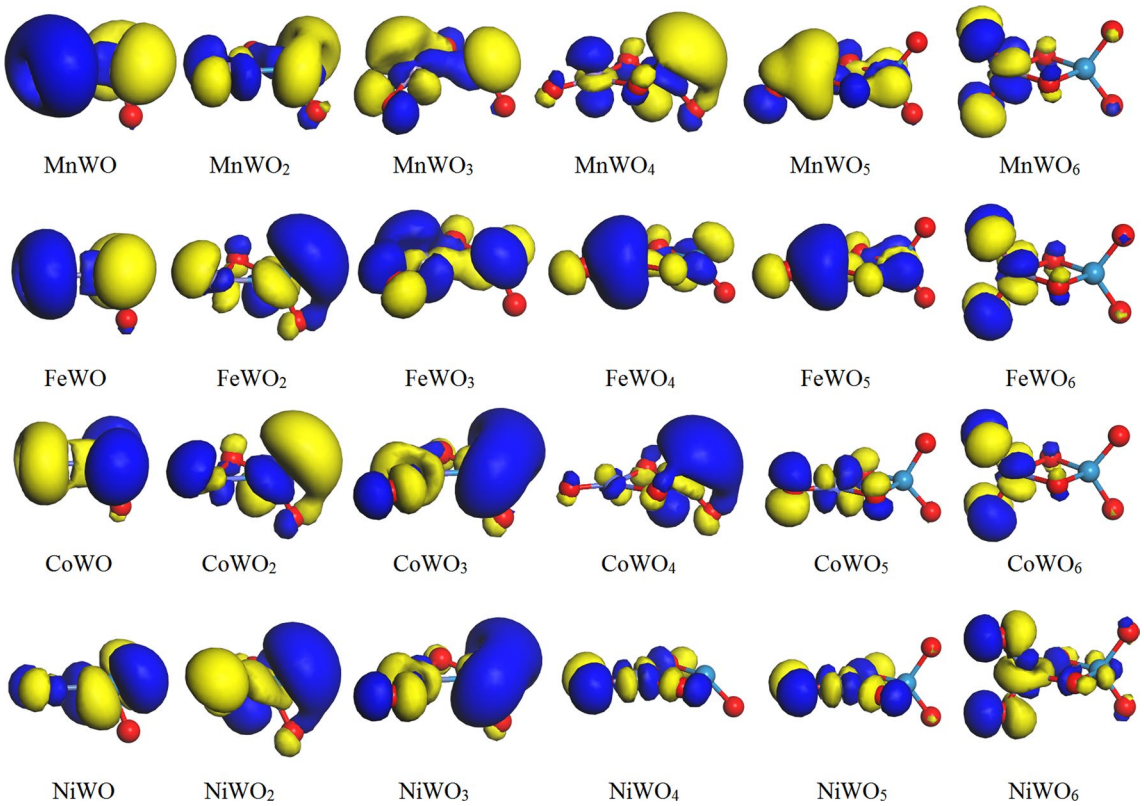

Fig. 5 LUMO orbitals of the $TMWO_n$ (TM = Mn, Fe, Co and Ni, n = 1–6) clusters

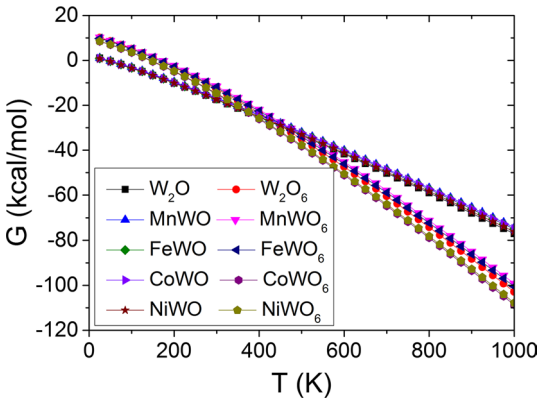

Fig. 6 Temperature dependence of the Gibbs free energy of the W_2O_n and $TMWO_n$ (TM = Mn, Fe, Co and Ni, n = 1, 6) clusters

The thermodynamical stability of the W_2O_n and $TMWO_n$ (TM = Mn, Fe, Co and Ni, n = 1–6) clusters can be analyzed by Gibbs free energy (*G*). The Gibbs free energies of the ground-state W_2O_n and $TMWO_n$ clusters have been plotted in Fig. 6. The Gibbs free energies of the W_2O_n and $TMWO_n$ clusters gradually decreases with the increase of the cluster size. It demonstrates that the W_2O_n and $TMWO_n$ clusters prefer to spontaneous grow with the increase of temperature. It demonstrates that the thermal stability of the W_2O_n and $TMWO_n$ clusters gradually increase with the increase of the cluster size. It results from the shell closing effect which obvious affects the activity of clusters [25].

3.3 Electronic attributes

The calculated Mülliken-charges of TM atoms of $TMWO_n$ (TM = Mn–Ni, n = 1–6) clusters have been plotted in Fig. 7. The amount of charge transferred between the TM atoms and WO_n clusters increases significantly as the number of oxygen atoms increases. This suggests that the W atoms become more positively charged with an increase in the number of O atoms. This indicates a conversion of the TM-O bond from a covalent bond to a partially ionic bond [1], which can help stabilize the remaining *d* electrons and increase their binding energies [10]. The amount of charge transferred of the $MnWO_n$ clusters is greater than in other $TMWO_n$ (TM = Fe, Co and Ni) clusters. While the amount in the $CoWO_n$ clusters is less than in other $TMWO_n$ clusters, except for the $NiWO_2$ clusters. The difference can be attributed to discrepancies in the electron affinity of the TM atoms [29, 30].

The natural electron configurations of TM atoms of $TMWO_n$ (TM = Mn–Ni, n = 1–6) clusters have been displayed in Table 1. Upon comparison of the valence electrons

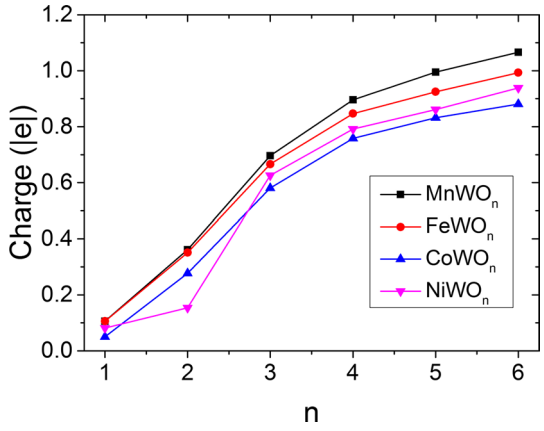

Fig. 7 Net-charges of TM atoms of the $TMWO_n$ (TM = Mn, Fe, Co and Ni, n = 1–6) clusters

Table 1 Natural electron configurations of TM (TM = Mn, Fe, Co and Ni) atoms for the $TMWO_n$ (TM = Mn, Fe, Co and Ni, n = 1–6) clusters

Cluster	Atom	Natural electron configuration
MnWO	Mn	[core]3p(6.006)3d(5.837)4s(0.925)4p(0.126)
$MnWO_2$	Mn	[core]3p(6.005)3d(5.742)4s(0.707)4p(0.182)
$MnWO_3$	Mn	[core]3p(5.996)3d(5.563)4s(0.450)4p(0.293)
$MnWO_4$	Mn	[core]3p(5.994)3d(5.497)4s(0.304)4p(0.307)
$MnWO_5$	Mn	[core]3p(5.991)3d(5.425)4s(0.263)4p(0.325)
$MnWO_6$	Mn	[core]3p(5.981)3d(5.318)4s(0.151)4p(0.490)
FeWO	Fe	[core]3p(6.004)3d(6.817)4s(0.969)4p(0.104)
$FeWO_2$	Fe	[core]3p(6.004)3d(6.754)4s(0.725)4p(0.164)
$FeWO_3$	Fe	[core]3p(5.997)3d(6.552)4s(0.490)4p(0.295)
$FeWO_4$	Fe	[core]3p(5.996)3d(6.489)4s(0.337)4p(0.329)
$FeWO_5$	Fe	[core]3p(5.994)3d(6.421)4s(0.301)4p(0.358)
$FeWO_6$	Fe	[core]3p(5.988)3d(6.324)4s(0.177)4p(0.521)
CoWO	Co	[core]3p(6.004)3d(7.819)4s(0.998)4p(0.128)
$CoWO_2$	Co	[core]3p(6.005)3d(7.785)4s(0.745)4p(0.186)
$CoWO_3$	Co	[core]3p(5.999)3d(7.560)4s(0.520)4p(0.338)
$CoWO_4$	Co	[core]3p(5.999)3d(7.507)4s(0.372)4p(0.362)
$CoWO_5$	Co	[core]3p(5.998)3d(7.430)4s(0.343)4p(0.397)
$CoWO_6$	Co	[core]3p(5.994)3d(7.327)4s(0.233)4p(0.566)
NiWO	Ni	[core]3p(6.002)3d(8.738)4s(1.069)4p(0.108)
$NiWO_2$	Ni	[core]3p(6.002)3d(8.725)4s(1.034)4p(0.084)
$NiWO_3$	Ni	[core]3p(6.000)3d(8.492)4s(0.547)4p(0.333)
$NiWO_4$	Ni	[core]3p(6.001)3d(8.458)4s(0.398)4p(0.350)
$NiWO_5$	Ni	[core]3p(6.000)3d(8.384)4s(0.365)4p(0.389)
$NiWO_6$	Ni	[core]3p(5.998)3d(8.278)4s(0.262)4p(0.523)

($3d^54s^2$, $3d^64s^2$, $3d^74s^2$ and $3d^84s^2$) of a single Mn, Fe, Co and Ni atom with those of $TMWO_n$ clusters, it can be observed that there is internal charge transfer of TM atoms of the $TMWO_n$ clusters from the 4*s* orbital to the 3*d* and 4*p* orbitals. Thus is evident in the Mülliken charges of the TM atoms of $TMWO_n$ clusters (See Fig. 6). This indicates that the 4*s* orbital electrons of the TM atoms for the $TMWO_n$ clusters are also partially transferred to the neighboring O atoms [13]. Similarly, there is internal charge transfer in the O atoms of the $TMWO_n$ clusters, with electrons from the 2*s* orbital being transferred to the 2*p* orbital [13]. This suggests that the 2*p* and 3*d* orbital electrons of the O atoms are obtained from the TM atoms.

3.4 Dipole magnitudes

Considering the high dipole moment leads to higher reactivity but less stability. The dipole magnitudes of the $TMWO_n$ (TM = Mn–Ni, n = 1–6) clusters have been displayed in Fig. 8. The nonzero dipole moments of the $TMWO_n$ clusters emerge. This is due to the symmetry of the W_2O_n clusters being degenerated by the TM substitution [35]. This is caused by insufficient hybridization between the TM-*d* electrons and O-*p* electrons of the $TMWO_n$ clusters. It causes the $TMWO_n$ (TM = Mn–Ni, n = 1–6) clusters display less structural stability. In general, the dipole moments of the $TMWO_n$ clusters decrease with the increase of the cluster sizes. It is due to the compensation effect of free electrons of O atoms on the dipole moments of $TMWO_n$ clusters. Similarly, the structural stability of the $TMWO_n$ clusters increases with the increase of the cluster sizes. The dipole magnitudes of the $MnWO_3$, $FeWO_2$, $CoWO_2$, $NiWO_2$ clusters are larger than those of neighboring $TMWO_n$ clusters.

4 Conclusions

The structures and electronic properties of the $TMWO_n$ (TM = Mn–Ni) clusters have been calculated using first-principles. The ground-state $TMWO_n$ clusters share some

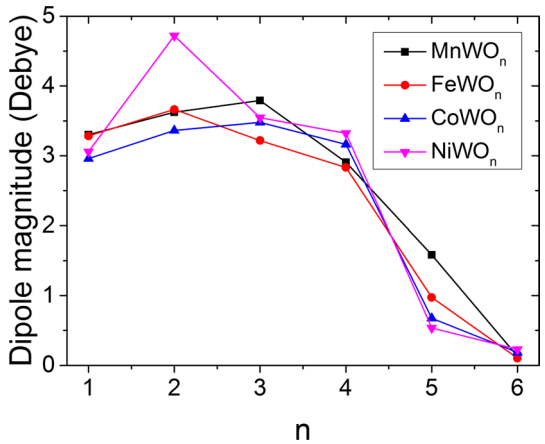

Fig. 8 Dipole magnitudes of the $TMWO_n$ (TM = Mn, Fe, Co and Ni, n = 1–6) clusters

structural similarities with the ground-state W_2O_n (n = 1–6) clusters. In the case of the $TMWO_2$ (TM = Fe–Ni) clusters, the W–O bonds are significantly distorted into a triangular structure. However, the $TMWO_n$ clusters are less thermodynamically stable compared to their corresponding W_2O_n clusters. The $NiWO_n$ (n = 1–2) and $CoWO_n$ (n = 3–5) clusters display greater thermodynamic stability than the other $TMWO_n$ clusters. Among the $TMWO_n$ clusters, the W_2O_4, W_2O_6, MnWO, $MnWO_3$, $MnWO_6$, FeWO, $FeWO_4$, $FeWO_6$, CoWO, $CoWO_6$, $NiWO_2$, $NiWO_5$ clusters are more kinetically stable. As the number of O atoms increases, there is a significant increase in the amount of charge transferred from 0.050 |e| to 1.066 |e| between the TM atoms and W_2O_n clusters. This charge transfer is highest in the $MnWO_n$ clusters compared to other $TMWO_n$ (TM = Fe, Co and Ni) clusters. The 4*s* orbital electrons of the TM atoms for the $TMWO_n$ clusters are also partially transferred to the neighboring O atoms. Additionally, the dipole magnitudes of the $MnWO_3$, $FeWO_2$, $CoWO_2$, $NiWO_2$ clusters are larger than those of neighboring $TMWO_n$ clusters.

Acknowledgements We gratefully acknowledge the financial support from the National Natural Science Foundation of China (Grant No. 51634004).

Author contributions ZL contributed to data curation, formal analysis, investigation, methodology, writing-original draft, writing-review and editing. ZHW contributed to investigation, writing-review and editing. ZZ contributed to funding acquisition, writing-review and editing.

Declarations

Conflict of interest The authors declare that they have no conflict of interest.

References

1. Sai L, Tang L, Huang X, Chen G, Zhao J, Wang J (2011) Chem Phys Lett 544:7
2. Valentin CD, Wang F, Pacchioni G (2013) Top Catal 56:1404
3. Jin H, Zhu J, Hu J, Li Y, Zhang Y, Huang X, Ding K, Chen W (2011) Theor Chem Acc 130:103
4. Kim YK, Dohnalek Z, Kay BD, Rousseau R (2009) J Phys Chem C 113:9721
5. Santo N, Filipescu M, Ossi PM, Dinescu M (2010) Appl Phys A 101:325
6. Li S, Dixon DA (2006) J Phys Chem A 110:6231
7. Sun Q, Rao BK, Jena P, Stolcic D, Kim YD, Gantefor G, Castleman AWJ (2004) J Chem Phys 121:9417
8. Zhai H-J, Kiran B, Cui L-F, Li X, Dixon DA, Wang L-S (2004) J Am Chem Soc 126:16134
9. Huang X, Zhai H-J, Li J, Wang L-S (2006) J Phys Chem A 110:85
10. Zhai H-J, Huang X, Cui L-F, Li X, Li J, Wang L-S (2005) J Phys Chem A 109:6019
11. Li D, Huang W-Q, Xie Z, Xu L, Yang Y-C, Hu W, Huang G-F (2016) Mod Phys Lett B 30:1650340
12. Xu L, Yin M-L, Liu S (2014) Sci Rep-UK 4:6745
13. Zhao Z, Wu Z, Li Z (2023) Struct Chem 34:1395
14. Hameed A, Gondal MA, Yamani ZH (2004) Catal Commun 5:715
15. Mansouri M, Mahmoodi T (2016) Acta Phys Pol A 129:8
16. Delley B (1990) J Chem Phys 92:508
17. Delley B (2000) J Chem Phys 113:7756
18. Li W, Da P, Zhang Y, Wang Y, Lin X, Gong X, Zheng G (2014) ACS Nano 8:11770
19. Zhao Z, Li Z, Xue G, Shen X, Wu J (2021) Mater Chem Phys 262:124272
20. Mulliken RS (1955) J Chem Phys 23:1841
21. Cora F, Patel A, Harrison NM, Dovesi R, Catlow CRA (1996) J Am Chem Soc 118:12174
22. Li Z, Shen X, Zhao Z (2022) Res Chem Intermediat 48:339
23. Baroni S, de Gironcoli S, Corso AD, Giannozzi P (2001) Rev Mod Phys 73:515
24. Fan J, Wang L-S (1995) J Chem Phys 102:8714
25. Geusic EM, Morse MD, Smalley RE (1985) J Chem Phys 82:590
26. Li Z, Zhou Z, Zhao Z, Wang Q (2018) Int J Mod Phys B 32:1850187
27. Wang S, Zhan J, Chen K, Ali A, Zeng L, Zhao H, Hu W, Zhu L, Xu X (2020) ACS Sustain Chem Eng 8:8214
28. Zhang J-M, Duan Y-N, Xu K-W, Ji V, Ma Z-Y (2008) Phys B 403:3119
29. Zhao L, Qu X, Wang Y, Lv J, Zhang L, Hu Z, Gu G, Ma Y (2017) J Phys: Condens Matter 29:265401
30. Zheng H, Ou JZ, Strano MS, Kaner RB, Mitchell A, Kalantar-zadeh K (2011) Adv Funct Mater 21:2175
31. Pan H, Wu Y, Li C, Li H, Gong Y, Niu L, Liu X, Sun CQ, Xu S (2022) Appl Surf Sci 571:151230
32. Ingham B, Hendy SC, Chong SV, Tallon JL (2005) Phys Rev B 72:075109
33. Zhao YR, Xu YQ, Chen P, Yuan YQ, Qian Y, Li Q (2021) Results Phys 26:104341
34. Zhang XY, Zhao YR, Li HX, Cheng KG, Liu ZR, Liu ZP, He H (2023) Chinese Phys B 32:066102
35. Li Z, Wu Z-H (2024). Surf Rev Lett. https://doi.org/10.1142/S0218625X24500392